ARTICLES

Electrochemical and Structural Studies on Microcrystals of the $(C_{60})_x$(CTV) Inclusion Complexes ($x = 1, 1.5$; CTV = cyclotriveratrylene)

Alan M. Bond,*,† Wujian Miao,† Colin L. Raston,† Timothy J. Ness,† Michael J. Barnes,† and Jerry L. Atwood‡

School of Chemistry, Monash University, Clayton, Victoria 3300, Australia, and Department of Chemistry, University of Missouri-Columbia, Missouri 65211

Received: August 2, 2000

The electrochemical reduction of microcrystals of $(C_{60})_x$(CTV) ($x = 1$, 1.5; CTV = cyclotriveratrylene) complexes adhered to electrode surfaces in contact with CH_3CN (0.10 mol L^{-1} Bu_4NClO_4) results in initial formation of $(C_{60}^-)_x$(CTV) which is followed by the liberation of the reduced fullerene anion from the CTV cavity. The released fullerene anion then reacts with the Bu_4N^+ electrolyte cation to form surface-confined $(Bu_4N)C_{60}$ species which can in turn be further reduced to solid-state and/or solution-phase multi-charged fullerene anions or oxidized to C_{60}(solid). The expelled CTV diffuses from the surface of the electrode into the bulk solution to form (Bu_4N^+)(CTV) species. The peak potential for one-electron reduction of solid $(C_{60})_x$-(CTV) is positively shifted by about 50 mV ($x = 1$) or 80 mV ($x = 1.5$) relative to the value for pure C_{60} microcrystals. These and results with other supramolecular complexes available in the literature suggest that the contact area between host and guest molecules as well as the position of high electron density area of the host are important factors that stabilize the host−guest complexes during/after the addition of electrons to the fullerene. The improved crystal structure determination of (C_{60})(CTV)$(toluene)_{0.5}$ using X-ray diffraction data at 173 K shows a two-dimensional close packed array of fullerenes with a third of these devoid of CTV.

Introduction

Fullerene C_{60} forms a wide range of supramolecular complexes with a variety of container molecules including azacrown ethers,[1] γ-cyclodextrin,[2,3] calixarenes,[4−15] and cyclotriveratrylene (CTV).[14,15] These complexes are of interest in material science,[16] biological applications,[16,17] and in separation science.[7,8,18,19] Recently, both solid-state and solution-phase electrochemical studies of these kinds of complexes[9,20−26] have been undertaken to explore the impact of the C_{60} redox level on the chemistry. In the present investigation, further structural details on the $(C_{60})_{1.5}$(CTV) complex are elucidated by X-ray crystallography, and electrochemical studies on microcrystals of supramolecular complexes of fullerene, $(C_{60})_x$(CTV) ($x = 1$, 1.5) complexes adhered to electrode surfaces, have been undertaken in order to explore the relationship between electrochemical behavior and the structure of host−guest complexes.

CTV (Figure 1a) is a macrocycle, possessing π-clouds arranged in a bowl shape, like calixarenes, albeit with greater rigidity, so that it can form two discrete complexes with C_{60} of composition $(C_{60})_x$(CTV), ($x = 1$, 1.5)[15,27] (Figures 1b and 2a). The structures of both complexes are dominated by fullerene−fullerene interactions, and each CTV has a C_{60} associated within the cavity of the CTV as a "ball-and-socket" nano-structure (Figure 1c). In the solid state, the 1:1 phase (C_{60})(CTV) complex has a polymeric zigzag array of fullerenes in the structure (Figure 1b). For the fullerene-rich phase $(C_{60})_{1.5}$(CTV) complex, the partial structure at least showed that the fullerenes collectively comprise a two-dimensional closed-pack array with 1/3 of the fullerenes devoid of CTV, and half of the solvent molecule of toluene for each $(C_{60})_{1.5}$(CTV) unit is also included in the crystal structure (Figure 2a).[14]

Because the (C_{60})(CTV) slowly decomposes in toluene[15] and both (C_{60})(CTV) and $(C_{60})_{1.5}$(CTV) complexes are readily degraded to their constituents in dichloromethane and chloroform,[15,27] the electrochemical studies of the complexes have been undertaken in the solid state in acetonitrile, in which C_{60} and the inclusion complexes are insoluble or only sparingly soluble[15,27,28] (see "Results and Discussion" below for details). Consistent with our previous electrochemical studies on solid C_{60}[29−31] and [$C_{60} \subset$ (*p*-benzylcalix[5]arene)$_2$],[32] microcrystalline samples of $(C_{60})_x$(CTV) ($x = 1$, 1.5) were directly adhered to the surface of the working electrodes, and Bu_4NClO_4 was used as the electrolyte.

Experimental Section

Chemicals. Acetonitrile, C_{60}, and Bu_4NClO_4 were used as in previous reports.[30−32] Crystalline $(C_{60})_x$(CTV) ($x = 1$, 1.5) complexes were prepared from a toluene solution containing a molar ratio 1:1 (for $x = 1$) or 10:1 (for $x = 1.5$) of CTV and C_{60}, respectively. On standing at 20 °C for 12−24 h, fine brown-black precipitates identified as (C_{60})(CTV) were produced from the former solution, and black crystalline plates of composition

* Corresponding Author. Tel: (+613) 9905 1338. Fax: (+613) 9905 4597. E-mail: a.bond@sci.monash.edu.au.
† Monash University.
‡ University of Missouri-Columbia.

10.1021/jp002768b CCC: $20.00
Published on Web 02/08/2001

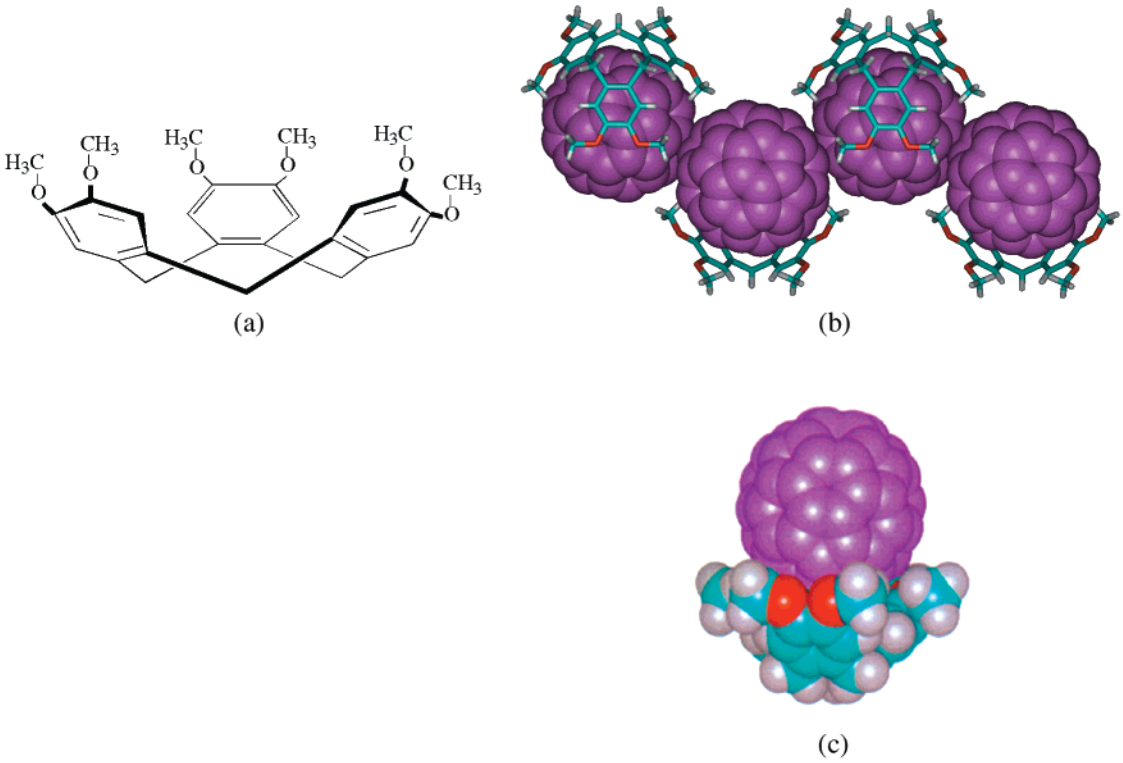

Figure 1. Structural details of (a) cyclotriveratrylene (CTV), (b) X-ray structure of (C_{60})(CTV), and (c) X-ray structure of the "ball-and-socket" nano-structure for $(C_{60})_x$ (CTV) ($x = 1$, 1.5).

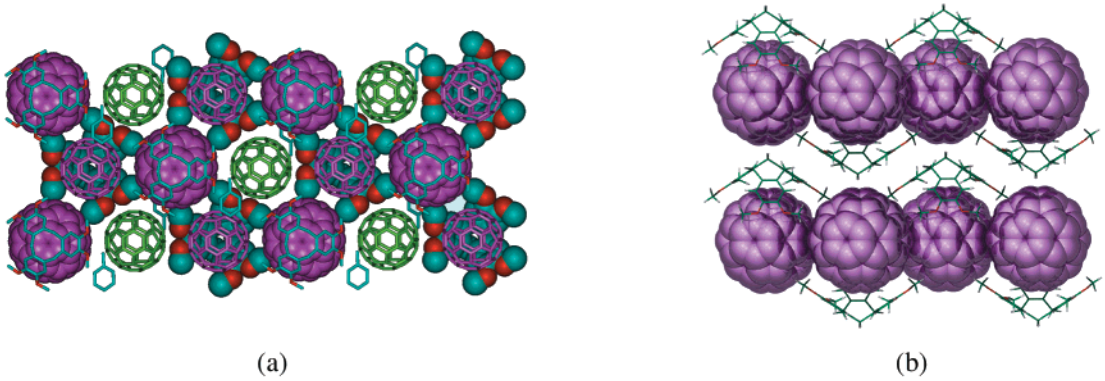

Figure 2. (a) Crystal packing of one layer of $(C_{60})_{1.5}$(CTV)$(toluene)_{0.5}$, idealized C_{60} molecules replace the disordered C_{60} molecules for clarity (green) and only on position is shown for each toluene molecule present; (b) Two layers of the crystal viewed side on, illustrating alternating CTV position with respect to C_{60}.

$(C_{60})_{1.5}$(CTV) were obtained in the latter case. More details concerning the preparation and characterization of these complexes are available in the literature.[7,15]

Electrochemical Instrumentation and Electrodes. Cyclic voltammetric experiments were undertaken with a Cypress Systems CS-2000 computerized instrument, using a 0.10 cm diameter glassy carbon as the working electrode. Microgravimetric experiments were performed on an Elchema EQCN-701 Electrochemical Quartz-crystal Nanobalance (Potsdam, New York), with 10 MHz gold-coated AT-cut quartz crystals (Bright Star Crystals, Vic, Australia) being used as working electrodes. The quartz-crystal and gold electrodes had diameters of 1.20 and 0.50 cm, respectively. Calibration procedures and assumptions associated with the use of the Sauerbrey equation to determine mass changes are provided in ref 32. With both forms of electrochemical instrumentation, Pt gauze and Ag/Ag^+ (0.010 mol L^{-1} $AgNO_3$ and 0.10 mol L^{-1} Bu_4NClO_4 in CH_3CN) were used as the counter and reference electrodes, respectively. The half wave potential of ferrocene/ferricinium couple was 0.082 V vs Ag/Ag^+ in CH_3CN (0.10 mol L^{-1} Bu_4NClO_4) solutions, with ferrocene added as an internal potential standard.

Micrographs were recorded with a HITACHI-2300 scanning electron microscope using an accelerating voltage of 20 kV. Samples were mounted on either a carbon conductive tab (Ted Pella, Inc., U.S.A.) or a gold-coated quartz-crystal electrode, and were gold coated in a Balzers sputter coating unit prior to microscopy. A Micromass Platform II electrospray mass spectrometer was used to acquire mass spectra.

The method for attachment of ground microcrystalline $(C_{60})_x$-(CTV) ($x = 1$, 1.5) complexes to the surface of working electrodes was the same as that described previously for the electrochemical studies of solid C_{60}[29−31] and C_{60}-calix[5]arene complex.[32]

All experiments were conducted under ambient temperature conditions of 20 ± 2 °C, and the electrolyte solutions (10 mL in cyclic voltammetry and 25 mL in quartz-crystal microgravimetry) were degassed with high purity N_2 for 5 min before the commencement of each experiment.

X-ray Diffraction Data Collection and Processing. Crystals of $(C_{60})_{1.5}$(CTV)(toluene)$_{0.5}$ were grown from toluene,[14] and because of apparent loss of solvent when removed from the mother liquor, crystals were mounted on a glass capillary under oil. Data were collected at 173(1) K on an Enraf-Nonius KappaCCD diffractometer with Mo-K_α radiation ($\lambda = 0.71073$ Å) then corrected for Lorentzian and polarization effects but not for absorption. The structure was solved by direct methods (SHELXS-97) and refined with a full matrix least-squares refinement on F^2 (SHELXL-97).[33] The well-ordered CTV and its cavity-bound C_{60} reside on a mirror plane. The uncomplexed C_{60} molecule and the toluene of solvation sit on *2/m* sites, and are highly disordered. The positions and refinement of the carbon atoms and their occupancies for this fullerene are consistent with the fullerene disordered over several positions around a common centroid. All non-hydrogen atoms were refined anisotropically, and hydrogen positions were located in the difference map and refined isotropically. $C_{120.5}H_{34}O_6$ $Mr =$ 1577.6, monoclinic, *C*2/*m*, $a = 30.1503(9)$, $b = 17.4125(5)$, $c = 14.4922(4)$ Å, $\beta = 116.37(1)$, $U = 6816.61(3)$ Å^3, $Z = 4$, $\rho_{calc} = 1.537$ g mol^{-1}, $\mu = 0.094$ mm^{-1} (no correction), $2\theta_{max} = 28.3°$, 7407 unique reflections, 1257 parameters, no restraints, $R_1 = 0.0803$ (3956 data $I > 2\sigma(I)$), $wR_2 = 0.2583$ (all data), $GoF = 1.055$. Crystallographic data (excluding structure factors) for this crystal structure has been deposited with the Cambridge Data Centre as supplementary publication number CCDC 138314. Copies of the data can be obtained free of charge on application to CCDC, 12 Union Road, Cambridge, CB21E2, U.K. (Fax: (+44) 1223-336-336-033. E-mail: deposit@ccdc.cam.ac.uk).

Results and Discussion

X-ray Crystal Structure Determination. The previously reported partial crystal structure of $(C_{60})_{1.5}$(CTV)(toluene)$_{0.5}$[27] has now been solved and refined using low temperature data. This has allowed a significant improvement on this structure, in the areas of location and refinement of atoms, especially of the disordered fullerene, and final R_1 room-temperature value. The structure contains one "ball-and-socket" supermolecule (C_{60})(CTV) unit which is ordered, as previously noted for the room-temperature data set (Figure 1c.), but now with greater position and lower thermal motion, and overall more meaningful bond distances and angles. The fullerene and CTV have a remarkable complementarity of curvature and must be one of the main factors in forming any complex from the outset. Moreover, the C_{60} is complexed by the CTV such that the 3-fold axes of the host molecule is aligned with a 3-fold symmetry axis of the fullerene. Thus two six-membered rings from either side of the C_{60} line up with the unique nine-membered ring of the CTV. Three five-membered rings of the fullerene adjacent to the six-membered ring residing immediately over the CTV are each positioned over one of the three aromatic rings of the CTV. This so-called symmetry matching optimizes the $\pi-\pi$ stacking between the five-membered rings on the fullerene and the CTV aromatics. We have recently noted that such symmetry matching is as an important consideration in designing host molecules for binding fullerenes.[34] In particular *p*-benzylcalix[5]arene forms a 1:2 complex with C_{60} where the two calixarenes completely shroud the fullerene, with the 5-fold symmetry axes of the calixarenes aligned with a 5-fold symmetry axis of the fullerene. In addition, *p*-benzylhexahomooxacalix[3]arene forms a similar 1:2 complex with the alignment of 3-fold symmetry axes, as in the present structure, albeit with only one host molecule associated with some of the fullerenes.[34]

The closest points of contact between the ordered C_{60} and CTV are consistent with a snug fit of the two interacting components at the van der Waals limit. Five-membered ring centoids of the fullerene to centroids of the six membered rings of the CTV range from 3.676 to 3.730 Å; the closest C...C contacts between the fullerene and the CTV are close to 3.40 Å as are the closest O(CTV)...C(fullerene) contacts. The C...C distances are similar to those reported for the structure of $(C_{60})_2$-(calix[6]arene),[35] which has a fullerene residing in each of the shallow cavities of the double cone conformation of the calixarenes, indeed with each fullerene-to-calixarene docking similar to the docking in the present structure.

The high level of dynamic disorder displayed by the uncomplexed C_{60} moiety, significantly more than for the room temperature determination,[14] prevented the elucidation of a coherent series of positions for the carbon atoms contained therein. The positions eventually used in the final refinement should be taken to be more indicative of a "rotating" shell of electron density than actual fixed carbon sites within the fullerene. The contrast of the disordered C_{60} with the complexed C_{60} molecule illustrates the degree of dynamic freedom allowed for the uncomplexed C_{60} in a space-filling role within the crystal lattice. Seemingly specific interactions, ideally over a large surface area with complementarity of curvature and symmetry matching, are needed to anchor a C_{60} residue in space, otherwise free rotation can prevail even at low temperatures. Interestingly, for the fullerene in the cavity, even at room temperature,[14] there is no disorder of the fullerene, which relates to complementarity of shape and $\pi-\pi$ interactions. In other complexes of C_{60}, for example the 1:1 complex with *p-tert*-butylcalix[8]arene,[36] there is free rotation of the fullerene in the solid at room temperature.

The packing within the crystal is dominated by inter-fullerene close contacts within two-dimensional arrays. The (C_{60})(CTV) nano-structure packs with the fullerenes in a hexagonal array around the disordered C_{60}, with the CTV alternating above and below adjacent fullerenes in each layer (Figure 2a). The centroid−centroid distance for the ordered fullerenes is 10.20 Å and the centroid−entroid distance between ordered and disordered fullerenes ranges from 10.09 to 10.10 Å, which are at the van der Waals limit and are unexceptional.[36] Individual carbon−carbon close contacts range from 3.65 to 3.69 Å between the ordered C_{60} molecules and approximately 3.40−3.70 Å between the ordered and disordered C_{60}'s. A small portion of one layer of fullerenes can be seen in Figure 2b, further illustrating the alternating position of the CTV relative to the C_{60} throughout the layer. Interactions between layers are limited to van der Waals interactions between the CTV molecules (exo- to their cavities) as they pack around the layers of C_{60} that run through the crystal. The sheets of C_{60} running through the lattice are another example of the many different types of interactions C_{60} displays in its supramolecular complexes, with double columns,[37−39] corrugated sheets,[40] and fully shrouded individual C_{60} molecules[34] being among other examples. The toluene of solvation found in the lattice acts in a space-filling role; being disordered over four sites, it is difficult to assign any specific interactions to the molecule.

Cyclic Voltammetry of Solid (C_{60})(CTV). Figure 3 shows cyclic voltammograms obtained over different potential ranges at a scan rate of 0.100 V s^{-1} for the reduction of solid (C_{60})-(CTV) mechanically adhered to a glassy carbon electrode and then placed in CH_3CN (0.10 mol L^{-1} Bu_4NClO_4). The previously elucidated cyclic voltammograms of solid C_{60} obtained under the same experimental conditions[31] also are displayed in Figure 3. Compared with solid C_{60}, one of the major differences

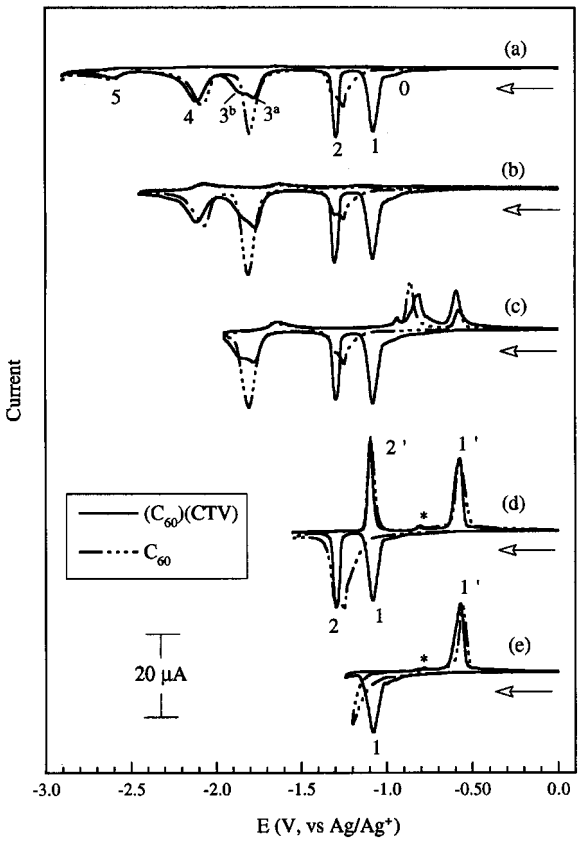

Figure 3. Cyclic voltammograms obtained over different potential ranges at a scan rate of 0.100 V s^{-1} for reduction of microcrystalline $(C_{60})(CTV)$ (—) and C_{60} (−··· −···) adhered to a 0.10 cm diameter glassy carbon electrode placed in CH_3CN (0.10 mol L^{-1} Bu_4NClO_4). (a) 0.000 to −2.900 V; (b) 0.000 to −2.450 V; (c) 0.000 to −1.950 V; (d) 0.000 to −1.550 V, and (e) 0.000 to −1.200 V vs Ag/Ag^+. (d, $i \times 2$ for C_{60}; e, $i \times 2.2$ for C_{60}).

in the voltammograms of solid $(C_{60})(CTV)$ complex is that the first two reduction processes are well resolved (processes 1 and 2, Figure 3a) even on the first cycle of the potential. The characteristics of symmetrical peak shapes and narrow peak widths ($\Delta E_{1/2} < 70$ mV) clearly revealed that both process 1 and process 2 are associated with the solid-state rather than solution-phase voltammetric responses. The prewave of process 1, which is designated as process 0 in Figure 3a, is believed to be associated with the dissolution of a small amount of neutral $(C_{60})(CTV)$ complex from the surface of the electrode, as proposed for the case of solid C_{60}.[41] When the potential direction was switched after process 1, a well-defined oxidation process 1′ was observed on the reverse scan (Figure 3e). The peak potential as well as peak shape of this process are very similar to those obtained for the oxidation of solid $(Bu_4N)C_{60}$ to C_{60}. Furthermore, a small "hump" (indicated by the symbol "*" in Figure 3e) also is a characteristic feature of the reduction of C_{60} "films"[42] or deposits[29] in CH_3CN containing Bu_4N^+ as the electrolyte. These observations imply that the $(C_{60})(CTV)$ complex may dissociate into C_{60} and CTV after addition of one electron. When the potential direction was switched after process 2, the reoxidation processes 2′ and 1′ (Figure 3d) exhibit peak potentials and peak shapes that are almost identical to those for solid C_{60}. Again, as expected, if dissociation occurred, a small "hump" that appeared between process 2′ and process 1′ was detected. It has been shown elsewhere[31] that the third reduction peak of solid C_{60} consisted of a mixture of both solid- and solution-based processes. Not surprisingly, if C_{60}^{2-} is formed after a two-electron reduction, when the potential was

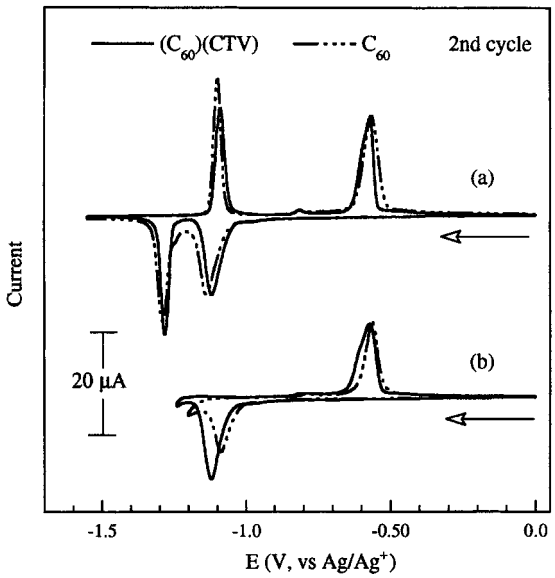

Figure 4. Second cycle of cycle voltammograms obtained over the potential range of (a) 0.000 to −1.550 V and (b) 0.000 to −1.200 V vs Ag/Ag^+ at a scan rate of 0.100 V s^{-1} for reduction of microcrystalline $(C_{60})(CTV)$ complex (—) and C_{60} (−··· −···) adhered to a 0.10 cm diameter glassy carbon electrode placed in CH_3CN (0.10 mol L^{-1} Bu_4NClO_4). (a, $i \times 1.74$ for C_{60}; b, $i \times 2.2$ for C_{60}).

scanned to the region of the $C_{60}^{2-/3-}$ reduction process, then two barely resolved processes 3^a and 3^b are observed (Figure 3a−c). Studies on solid C_{60} in CH_2Cl_2[43] established that the one-electron redox processes of solution-phase C_{60} occurred at significantly less negative potential values than those of the solid-state redox couple. Processes 3^a and 3^b in Figure 3a therefore are believed to be associated with the solution-phase and solid-state reductions of two-electron reduced C_{60}^{2-} species to three-electron reduced species, respectively. Processes 4, 5 and all waves on the reverse scans essentially have the same characteristics as those found in the reduction of solid C_{60} (Figure 3a−e).

Continuous cycling over the potential region of the first redox couple or over both the first and second couples generates a relatively long-lasting "steady-state" voltammetric response. Figure 4 shows an example of such an experiment, where both peak potentials and peak shapes for solid $(C_{60})(CTV)$ complex are now close to those for solid C_{60}. The peak potential for the process 1 is shifted negatively by about 50 mV in the second cycle of the potential. This result further supports the deduction based on the initial experiments (Figure 3) that the $(C_{60})(CTV)$ complex dissociates to C_{60}^- and CTV after the one-electron reduction.

Very similar cyclic voltammograms were observed when solid $(C_{60})(CTV)$ complex was adhered to a gold electrode instead of a glassy carbon and placed in CH_3CN (0.10 mol L^{-1} Bu_4NClO_4), as was the case for solid C_{60}.[31] Thus, the results of microgravimetric studies described below using the EQCM method with gold electrodes therefore are presumed to be valid for both electrode surfaces.

Microgravimetry on the Reduction of the Solid (C_{60})-(CTV) Complex. If the reactions postulated above are correct, then significant mass changes should accompany the reduction of $(C_{60})(CTV)$. Detection of these anticipated mass changes was undertaken by the electrochemical quartz-crystal microbalance (EQCM) method in order to provide additional mechanistic details.

Figure 5 shows the mass change−time transients for solid $(C_{60})(CTV)$ complex and C_{60} adhered to a gold quartz-crystal

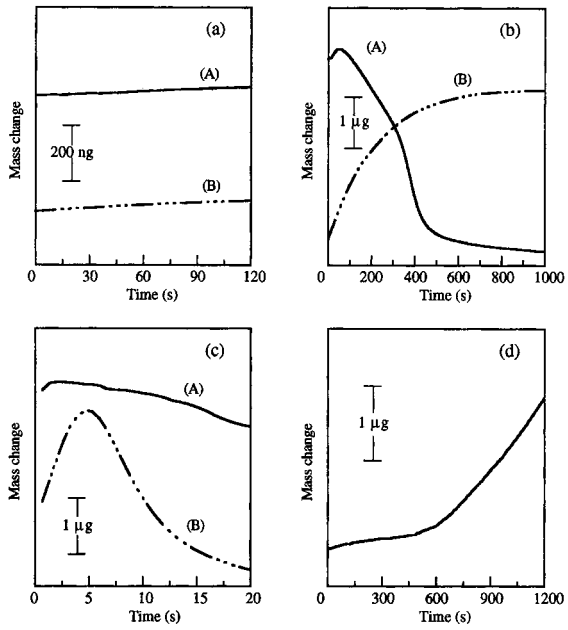

Figure 5. Microgravimetric EQCM experiments on microcrystalline (C_{60})(CTV) complex (A, —) and C_{60} (B, —··· —···) adhered to a 0.50 cm diameter Au/QC electrode placed in CH_3CN (0.10 mol L^{-1} Bu_4NClO_4) (a−c) or saturated CTV/CH_3CN (0.10 mol L^{-1} Bu_4NClO_4) (d) at (a) at the open-circuit potential, (b) −1.200 V, (c) −1.550 V and (d) −1.200 V vs Ag/Ag^+.

(Au/QC) electrode placed in CH_3CN (0.10 mol L^{-1} Bu_4NClO_4) under the specified potentiostated conditions. Only very small mass gains (<35 ng in 120 s) were observed over long periods of time at open circuit potential for the (C_{60})(CTV) complex (Figure 5a(A)) and C_{60} (Figure 5a(B)), confirming that both of these solids are essentially insoluble in acetonitrile. However, the results of these experiments suggest that traces of solvent and/or electrolyte may be gradually adsorbed or trapped onto (C_{60})(CTV)- and C_{60}-coated Au/QC electrode surfaces. In contrast, when the potential was stepped to −1.200 V vs Ag/Ag^+ and then held at this value, the first reduction process for the (C_{60})(CTV) complex occurs with an initially small mass increase (first 50 s) followed by a significant mass loss (Figure 5b(A)). This sequence of mass changes is consistent with the presence of the reaction scheme

$$\underset{\text{(solid)}}{(C_{60})(CTV)} + \underset{\text{(soln)}}{Bu_4N^+} \xrightarrow{+e^-} \underset{\text{(solid)}}{[Bu_4N^+][(C_{60}^-)(CTV)]} \xrightarrow{\text{fast}} \underset{\text{(solid)}}{[Bu_4N^+][C_{60}^-]} + \underset{\text{(soln)}}{CTV} \quad (1)$$

Thus, the initial mass gain in Figure 5b(A) is attributed to the formation of a transient $[Bu_4N^+][(C_{60}^-)(CTV)]$ (solid) species, which then loses CTV. Since CTV is very soluble in acetonitrile and its molecular weight (450 g mol^{-1}) is significantly larger than that of Bu_4N^+ (242 g mol^{-1}), an overall mass loss of 208 g (per mole of electron transfer) is expected according to eq 1. However, the dissolution of initially surface-confined CTV into the bulk of the electrolyte solution could "undermine" unreacted (C_{60})(CTV) (solid) or newly formed $(Bu_4N)C_{60}$ (solid), giving larger mass losses than predicted solely on the basis of reductive electrolysis.[44] In very long-time experimental scales (>1200 s, not shown), the mass becomes constant.

In contrast to the overall mass loss found after reduction of (C_{60})(CTV), the one-electron reduction of solid C_{60} to C_{60}^- leads to a significant mass increase (Figure 5b(B)) due to the reaction[45]

$$C_{60}(solid) + Bu_4N^+(soln) \xrightarrow{+e^-} (Bu_4N)C_{60}(solid) \quad (2)$$

In the case of adhered microcrystals of C_{60}, after about 700 s, the mass also approaches a constant value, when reaction 2 is completed because the C_{60}^- product is almost insoluble in acetonitrile. A similar result also has been observed in the case of C_{60} "films".[42]

When the potential was stepped to −1.550 V vs Ag/Ag^+, an overall two-electron reduction process occurs and the reaction scheme can be described as

$$(C_{60})(CTV)(solid) + 2Bu_4N^+(soln) \xrightarrow{+2e^-} [Bu_4N^+]_2[C_{60}^{2-}](solid) + CTV(soln) \quad (3)$$

This equation requires that a slight increase in mass (34 g per two-mole electron transfer) should occur with time. However, the experimental result (Figure 5c(A)) shows that except for the first 2 s, where a slight mass gain is indeed observed, that a slow mass loss occurs for the remainder of the time. This behavior is assigned to both the "undermining" effect noted above associated with dissolution of CTV and to slow dissolution of $[Bu_4N^+]_2[(C_{60}^{2-})]$ (solid) as also evidenced in Figure 5c-(B) when solid C_{60} is reduced to C_{60}^{2-} via a reaction scheme of the kind[46]

$$C_{60}(solid) + 2Bu_4N^+(soln) \xrightarrow{+2e^-} [Bu_4N^+]_2[C_{60}^{2-}](solid) \xrightarrow{\text{slow}} C_{60}^{2-}(soln) + 2Bu_4N^+(soln) \quad (4)$$

If the reaction in scheme (1) is operative, and a saturated CTV acetonitrile (0.10 mol L^{-1} Bu_4NClO_4) solution is present, then the one-electron reduction of solid (C_{60})(CTV) to $[Bu_4N^+][(C_{60}^-)(CTV)]$ at − 1.200 V vs Ag/Ag^+ should give rise to an increase rather than loss in mass, because dissolution of CTV from the solid into solution will be prevented, while uptake of the electrolyte cation into the solid still occurs. Indeed, as shown in Figure 5d, in the presence of a saturated CTV solution, a small mass gain is detected for the first 500 s. This slow increase is followed by a rapid increase in mass for the next 700 s. However, the total mass gain of ca. 2.0 μg in the initial 1200 s is clearly much larger than the value of 0.83 μg calculated on the basis of an initial (C_{60})(CTV) coverage of ca. 4.0 μg detected from data in Figure 5b where all solid is removed from the surface. More importantly, there is no indication of the mass increase stopping even after a 1200 s period of one-electron reduction. This implies that an other process involving incorporation of CTV onto the surface may occur on long time scales when the complex is placed in the solution phase. As a controlled experiment it was shown that no significant mass change was observed for the one-electron reduction of solid C_{60} in the presence of a saturated solution of CTV in acetonitrile (0.10 mol L^{-1} Bu_4NClO_4).

Identification of (Bu_4N^+)(CTV) Species Formed on Electrode Surfaces after the One-Electron Reduction Process. (C_{60})(CTV) forms star- and needle-type crystals (Figure 6a). A SEM image is shown in Figure 6b for (C_{60})(CTV) complex adhered to a Au/QC electrode after electrochemical reduction at − 1.200 V vs Ag/Ag^+ for 300 s when the electrode is placed in CH_3CN (0.10 mol L^{-1} Bu_4NClO_4). It is evident that a few (C_{60})(CTV) crystals with roughened surfaces remain on the surface after this time, suggesting that electrochemical conversion processes associated with reduction are relatively slow as

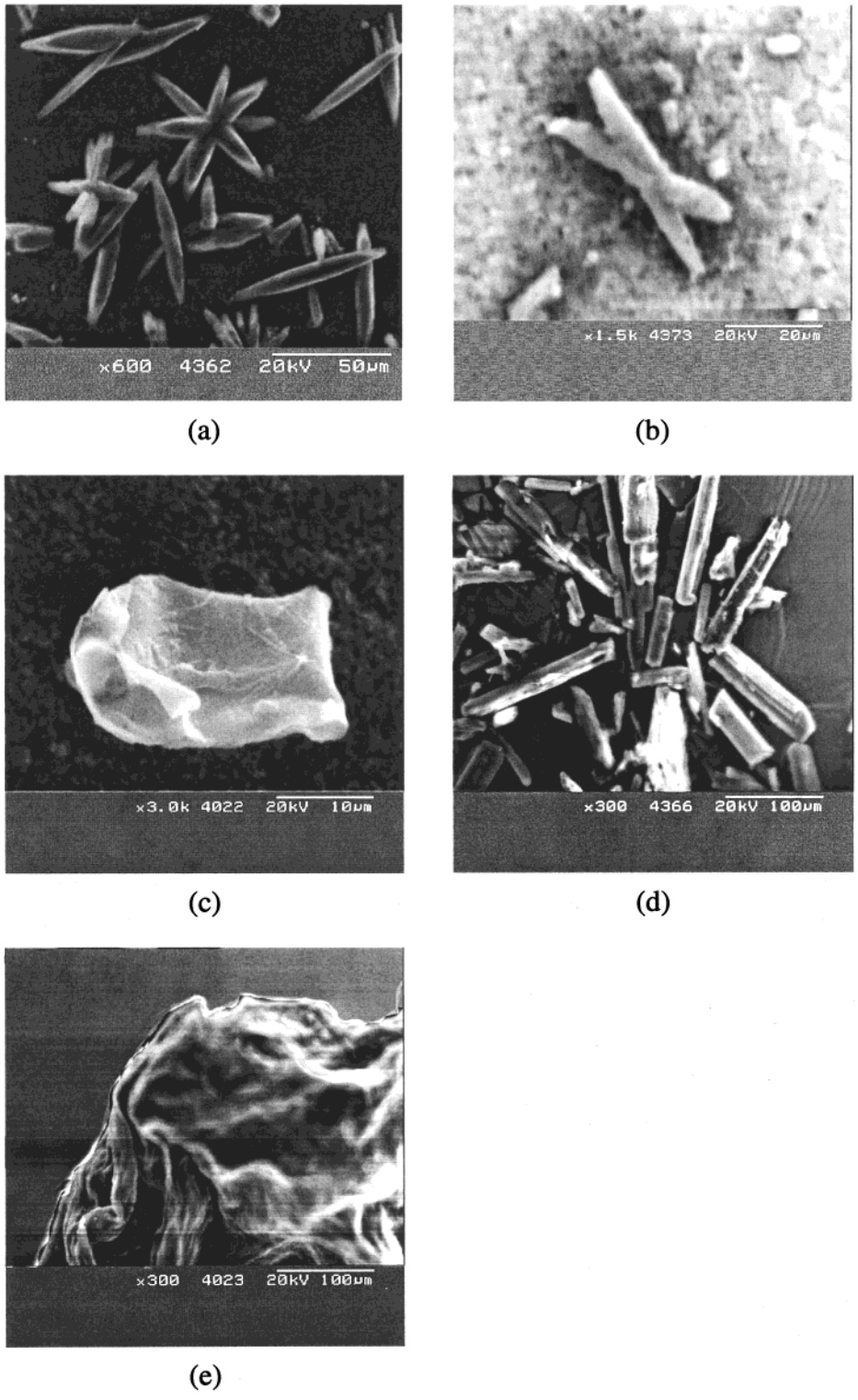

Figure 6. SEM images shown for (a) (C_{60})(CTV) crystals on a carbon conductive tab, (b) (C_{60})(CTV) crystallites on a Au/QC electrode after the potential was held at −1.200 V vs Ag/Ag^+ for 300 s in CH_3CN containing 0.10 mol L^{-1} Bu_4NClO_4, (c) (C_{60})(CTV) adhered to a Au/QC electrode placed in a saturated CTV/CH_3CN (0.10 mol L^{-1} Bu_4NClO_4) after the potential was held at −1.200 V vs Ag/Ag^+ for 1200 s, (d) CTV crystals on a carbon conductive tab, and (e) precipitate obtained from a nearly saturated 12 mmol L^{-1} CTV/CH_3CN (0.10 mol L^{-1} Bu_4NClO_4) solution on a carbon conductive tab.

expected on the basis of data obtained by cyclic voltammetry (Figure 3) and microgravimetry (Figure 5b).

Figure 6c shows a SEM image obtained for (C_{60})(CTV) complex adhered to a Au/QC electrode placed in a saturated CTV solution in acetonitrile (0.10 mol L^{-1} Bu_4NClO_4) after the one-electron electrochemical reduction had occurred at −1.200 V vs Ag/Ag^+ for 1200 s (cf. Figure 5d). Before the SEM measurement was made, the specimen was washed with CH_3CN to remove all material soluble in this solvent. Clearly, the newly formed solid "film" is not unreacted (C_{60})(CTV) (Figs. 6a and b), and is unlikely to be CTV either (Figure 6d).

It was known that the electrolyte Bu_4N^+ cation has a similar size to C_{60}, notably a globular species of 10 Å in diameter,[47,48] and that the upper rim of the CTV molecule has high electron

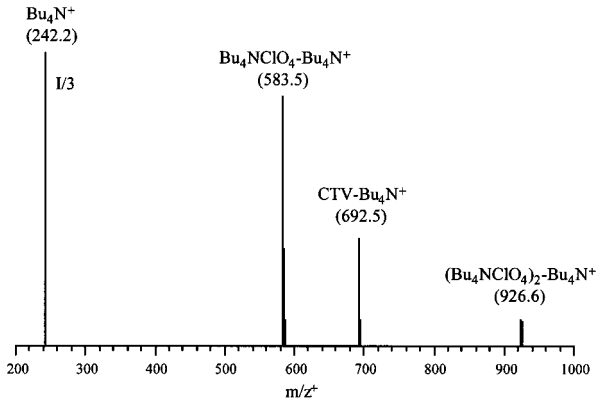

Figure 7. Electroscopy mass spectra obtained using the positive ion detection mode for a nearly saturated CTV/CH_3CN (0.10 mol L^{-1} Bu_4NClO_4) solution after a 100-fold dilution with acetonitrile.

density (Figure 1a). Consequently, the Bu_4N^+ cation also may be able to form a CTV complex in acetonitrile (eq 5):

$$Bu_4N^+ + CTV \xrightarrow{CH_3CN} (Bu_4N^+)(CTV) \qquad (5)$$

To support this hypothesis, a nearly saturated 12 mmol L^{-1} CTV acetonitrile solution containing 0.10 mol L^{-1} Bu_4NClO_4 was prepared. About 2 h later, white cotton-wadding-like precipitates appeared. SEM examination of the solid revealed that these precipitates exhibited a film-like appearance (Figure 6e), with a similar image to the material formed on the electrode after reduction of (C_{60})(CTV) in a saturated CTV solution (Figure 6c). Further evidence for the formation of a (Bu_4N^+)(CTV) species was obtained using electrospray mass spectrometry. An electroscopy mass spectrum (positive ion detection mode) of a 100-fold diluted (with acetonitrile) CTV/Bu_4NClO_4 solution is shown in Figure 7. The major peaks with 242.2, 583.5, 692.5, and 924.8 m/z^+ are attributed to Bu_4N^+, $(Bu_4NClO_4)-Bu_4N^+$, (Bu_4N^+)(CTV), and $(Bu_4NClO_4)_2-Bu_4N^+$ species, respectively. No m/z^- peak related to $(ClO_4^-)_n$(CTV) ($n = 1, 2, 3, 4$) species was observed in a negative ion mode electroscopy mass spectrum. Thus, the film shown in Figure 6c is probably a (Bu_4N^+)(CTV) perchlorate salt, which gives rise to the continuous increase in mass observed at long times under the conditions of Figure 5d.

Cyclic Voltammetry and Microgravimetry (EQCM) of Solid $(C_{60})_{1.5}$(CTV) Complex. Cyclic voltammograms for the reduction of solid $(C_{60})_{1.5}$(CTV) complex in CH_3CN (0.10 mol L^{-1} Bu_4NClO_4) are very similar to those for the (C_{60})(CTV) complex (compare Figures 8 and 3). Both sets of voltammograms exhibit well-resolved first and second one-electron reduction waves, and a split or broad third reduction process. However, two aspects of the voltammetry reflect the internal structural differences. First, in the initial potential cycle, the $(C_{60})_{1.5}$(CTV) reduction peak potentials for processes 1 and 2 occurred at less negative values by about 30 and 20 mV, respectively, compared to the corresponding peak potentials for the reduction of (C_{60})(CTV) complex. Second, when the potential was cycled over the region of the first two pairs or the first pair of redox couples, only one small "hump" between processes 1 and 1′ (indicated as "*" in Figure 3d,e) was observed for (C_{60})(CTV) complex (Figures 3d,e and 4), while two "humps" were evident for $(C_{60})_{1.5}$(CTV) (Figure 8d,d′,e,e′). However, with $(C_{60})_{1.5}$(CTV), the "hump" with the relatively less negative oxidation peak potential and broader wave shape disappeared, while the remaining "hump" remained essentially the same as the small response obtained for the reduction of

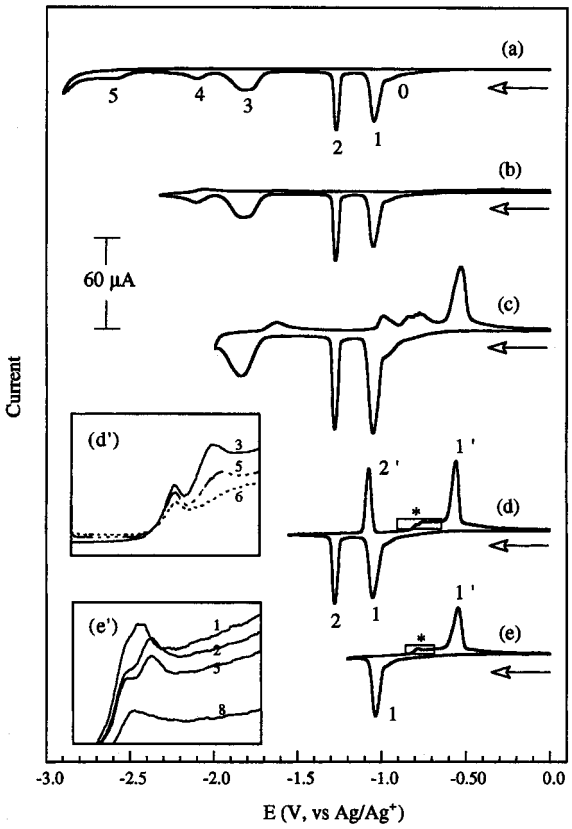

Figure 8. Cyclic voltammograms obtained over different potential ranges at a scan rate of 0.100 V s^{-1} for reduction of microcrystalline $(C_{60})_{1.5}$(CTV) complex adhered to a 0.10 cm diameter glassy carbon electrode placed in CH_3CN (0.10 mol L^{-1} Bu_4NClO_4). (a) 0.000 to −3.000 V; (b) 0.000 to −2.350 V; (c) 0.000 to −2.000 V; (d) 0.000 to −1.550 V and (e) 0.000 to −1.200 V vs Ag/Ag^+. See main text for the description of inserts (d′) and (e′).

solid C_{60} or (C_{60})(CTV) complex after about 5 to 7 cycles (Figure 8d′,e′). The numbers 1, 2, ..., 8 shown in Figure 8 d′,e′ refer to the number of potential cycles. As was the case with solid C_{60},[41] this "hump" is believed to be associated with the oxidation of a very small concentration of dissolved C_{60}-species. It was known that half a toluene molecule in each $(C_{60})_{1.5}$(CTV) unit is included in the crystal structure (Figure 2a), and that C_{60} is soluble in toluene.[28] Consequently, the two "humps" shown in Figure 8d′,e′ may be attributed to reactions of the kind,[44]

$$C_{60}^-(soln) \xrightarrow{-e^-} C_{60}(solid) \qquad (6)$$

$$C_{60}^-(soln) \xrightarrow{-e^-} C_{60}(soln) \qquad (7)$$

In accordance with this scheme it would be predicted that the initially included toluene molecules gradually would be diffused/expelled from the surface-attached solid into the bulk solution after extended periods of potential cycling, thereby explaining why the electrochemical response associated with reaction 7 progressively became smaller and then eventually disappeared.

The fact that the cyclic voltammetric technique does not provide separate processes for the two different chemical states of C_{60} that exist in the crystal structure of $(C_{60})_{1.5}$(CTV) complex (Figure 2a), presumably reflects the fact that the interaction forces between C_{60}−CTV, C_{60}−C_{60}, and $(C_{60}$−CTV)−C_{60} are very similar.

Microgravimetric (EQCM) results for the reduction of $(C_{60})_{1.5}$-(CTV) complex adhered to a Au/QC electrode placed in CH_3-

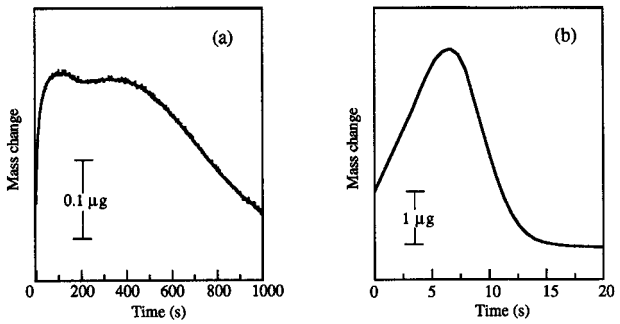

Figure 9. Microgravimetric EQCM experiments on microcrystalline $(C_{60})_{1.5}$(CTV) adhered to a 0.50 cm diameter Au/QC electrode placed in CH_3CN (0.10 mol L^{-1} Bu_4NClO_4) at a potential of (a) −1.200 V, (b) −1.550 V vs Ag/Ag^+.

CN (0.10 mol L^{-1} Bu_4NClO_4) at −1.200 V (one-electron process) and −1.550 V vs Ag/Ag^+ (two-electron process) are shown in Figure 9a,b, respectively. At −1.200 V, a period of mass gain (first 100 s) is followed by one of slower mass decrease (next 900 s) (Figure 9a). This behavior is consistent with the mechanism

$$\frac{2}{3}[(C_{60})_{1.5}(CTV)](solid) + Bu_4N^+(soln) \xrightarrow{+e^-}$$

$$\left\{\left[\frac{2}{3}(C_{60}^-)_{1.5}(CTV)\right](Bu_4N^+)\right\}(solid) \rightarrow$$

$$(Bu_4N)C_{60}(solid) + \frac{2}{3}CTV(soln) \quad (8)$$

An overall 58 g mass loss (per mole of electron transfer) is calculated on the basis of eq 8, which is significantly smaller than the 208 g mass loss predicted for the one-electron reduction of (C_{60})(CTV) to $(Bu_4N)C_{60}$ (solid) (eq 1), and thus the experimental data (Figure 9a vs Figure 5b) qualitatively follow this theoretical expectation. When the potential was held at −1.550 V vs Ag/Ag^+, the reaction scheme (eq 9) is expected to occur:

$$\begin{array}{l} \frac{2}{3}[(C_{60})_{1.5}(CTV)](solid) + 2Bu_4N^+(soln) \xrightarrow{+2e^-} (Bu_4N)_2C_{60}(solid) + \frac{2}{3}CTV(soln) \\ \qquad\qquad\qquad\qquad\qquad\qquad\qquad\qquad\qquad\qquad \downarrow \text{slow} \\ \qquad\qquad\qquad\qquad\qquad\qquad\qquad\qquad\qquad\qquad 2Bu_4N^+(soln) + C_{60}^{2-}(soln) \end{array} \quad (9)$$

In the absence of dissolution of $(Bu_4N)_2C_{60}$ (solid) to C_{60}^{2-}(soln), a 185 g mass gain (per two moles of electron transfer) is expected to be produced, which is much larger than the 34 g calculated for the two-electron reduction of (C_{60})(CTV) to $(Bu_4N)_2C_{60}$ (solid) (eq 3). Not surprisingly, the experimentally observed mass change−time transient exhibited an initial large mass increase (first 7 s), while at longer times the dissolution process became dominant and is associated with a period of large mass loss.

Conclusions

The electrochemical reduction of microcrystals of the $(C_{60})_x$-(CTV) ($x = 1$, 1.5) complexes adhered to electrodes placed in CH_3CN (0.10 mol L^{-1} Bu_4NClO_4) leads to initial formation of $(C_{60}^-)_x$(CTV) which is followed by the liberation of the reduced fullerene anion from the CTV cavity. The released fullerene anion then reacts with the Bu_4N^+ electrolyte cation to form surface confined $(Bu_4N)C_{60}$ species which can in turn be further reduced to solid-state and/or solution-phase multi-charged fullerene anions or oxidized to C_{60}(solid). The expelled CTV diffuses from the surface of the electrode into the bulk solution to form (Bu_4N^+)(CTV) complexes. The peak potential for one-electron reduction of solid $(C_{60})_x$(CTV) is positively shifted by about 50 mV ($x = 1$) or 80 mV ($x = 1.5$) relative to the value for pure C_{60} microcrystals.

Since the electrochemical behavior of solid [$C_{60} \subset$ (*p*-benzylcalix[5]arene)$_2$] complex[32] does not lead to free reduced C_{60} anions during the course of one-electron reduction, it is likely that the contact area between host and guest molecules as well as the position of high electron density area of the host are important factors that stabilize the host−guest complexes during/after the addition of electrons to the fullerene. In the structure of [$C_{60} \subset$ (*p*-benzylcalix[5]arene)$_2$] complex, most of the surface of the fullerene is shrouded by two *p*-benzylcalix[5]arene molecules,[34] while in $(C_{60})_x$(CTV) ($x = 1$, 1.5) only a small part of the fullerene is in the cavity of the CTV (Figure 1b).[14,15,27] The high electron density area of the host could become the target for attack of electrolyte cations during/after the reduction of complexes. In the case of [$C_{60} \subset$ (*p*-benzylcalix-[5]arene)$_2$] complex, the high electron density area is on the lower rim of the calixarene, whereas in the case of $(C_{60})_x$(CTV) ($x = 1$, 1.5), the high electron density area is on the upper rim of the CTV.

Acknowledgment. The authors gratefully acknowledge the Australian Research Council for financial support of this project.

References and Notes

(1) Diederich, F.; Effing, J.; Jonas, U.; Jullien, L.; Plesnivy, T.; Ringsdorf, H.; Weinstien, D. *Angew. Chem., Int. Ed. Engl.* **1993**, *31*, 1599.
(2) Zhang, D. D.; Liang, Q.; Chen, J. W.; Li, M. K.; Wu, S. H. *Supramol. Chem.* **1994**, *3*, 325.
(3) Andersson, T.; Nilsson, K.; Sundahl, M.; Westman, G.; Wennerstrom, O. *Chem. Commun.* **1992**, 604.
(4) Shinka, S. *Chem. Commun.* **1994**, *22*, 2586.
(5) Williams, R. M.; Verhoeven, J. M. *Recl. Trav. Chim. Pay-Bas.* **1992**, *111*, 531.
(6) Williams, R. M.; Zwier, J. M.; Verhoeven, J. W.; Nachtegoal, G. H.; Kentgens, A. P. M. *J. Am. Chem. Soc.* **1994**, *116*, 6965.
(7) Atwood, J. L.; Koustantonis, G. A.; Raston, C. L. *Nature* **1994**, *368*, 229.
(8) Suzuki, T.; Nakashima, K.; Shinkai, S. *Chem. Lett.* **1994**, 699.
(9) Chen, Z.; Fox, J. M.; Gale, P. A.; Beer, P. D.; Rosseinsky, M. J. *J. Electroanal. Chem.* **1995**, *392*, 101.
(10) Castillo, R.; Ramos, S.; Cruz, R.; Martinez, M.; Lara, F.; Ruiz-Garcia, J. *J. Phys. Chem.* **1996**, *100*, 709.
(11) Suzuki, T.; Nakashima, K.; Shinkai, S. *Tetrahedron Lett.* **1995**, *36*, 249.
(12) Isaacs, N. S.; Nichols, P. J.; Raston, C. L.; Sandoval, C. A.; Young, D. J. *Chem. Commun.* **1997**, 1839.
(13) Raston, C. L.; Atwood, J. L.; Nichols, P. J.; Sudria, I. B. N. *Chem. Commun.* **1996**, 2615.
(14) Hardie, M. J.; Raston, C. L. *Chem. Commun.* **1999**, 1193.
(15) Atwood, J. L.; Barnes, M. J.; Gardiner, M. G.; Raston, C. L. *Chem. Commun.* **1996**, 1449.
(16) Baum, H. R. M. In *Chem. Eng. News* **1993**, *71* (47), 8.
(17) Friendman, S. H.; DeCamp, D. L.; Sijbesma, R. P.; Srdanov, G.; Wudl, F.; Kenyon, G. *J. Am. Chem. Soc.* **1993**, *115*, 6506.
(18) Diederich, F.; Rubin, Y. *Angew. Chem., Int. Ed. Engl.* **1992**, *31*, 1101.
(19) Taylor, R.; Walton, D. R. M. *Nature* **1993**, *363*, 685.
(20) Boulas, P.; Kutner, W.; Jones, M. T.; Kadish, K. M. *J. Phys. Chem.* **1994**, *98*, 1282.
(21) Cliffel, D. E.; Bard, A. J.; Shinkai, S. *Anal. Chem.* **1998**, *70*, 4146.
(22) Luo, H. X.; Li, N. X.; He, W. J.; Shi, Z. J.; Gu, Z. N.; Zhou, X. H. *Electroanalysis* **1998**, *10*, 576.
(23) Li, N. Q.; Zhou, B.; Luo, H. X.; He, W. J.; Shi, Z. J.; Gu, Z. N.; Zhou, X. H. *J. Solid State Electrochem.* **1998**, *2*, 253.
(24) Li, M. X.; Li, N. Q.; Gu, Z. N.; Sun, Y. L.; Wu, Y. Q. *Electroanalysis* **1997**, *9*, 490.
(25) Li, M. X.; Li, N. Q.; Gu, Z. N.; Zhou, X. H.; Sun, Y. L.; Wu, Y. Q. *Electrochim. Acta* **1996**, *41*, 2897.
(26) Olsen, S. A.; Bond, A. M.; Compton, R. G.; Lazarev, G.; Mahon, P. J.; Marken, F.; Raston, C. L.; Tedesco, V.; Webster, R. D. *J. Phys. Chem. A* **1998**, *102*, 2641.

(27) Steed, J. W.; Junk, P. C.; Atwood, J. L.; Barnes, M. J.; Raston, C. L. *J. Am. Chem. Soc.* **1994**, *116*, 10346.
(28) Ruoff, R. S.; Tse, D. S.; Malhotra, R.; Lorents, D. C. *J. Phys. Chem.* **1993**, *97*, 3379.
(29) Suarez, M. F.; Marken, F.; Compton, R. G.; Bond, A. M.; Miao, W. J.; Raston, C. L. *J. Phys. Chem. B* **1999**, *103*, 5637.
(30) Bond, A. M.; Oldham, K. B.; Miao, W. J.; Feldberg, S. W.; Raston, C. L. In *Sixth International Seminar on Electroanal. Chem. (Extended Abstracts)*; Chinese Chemical Society: Changchun, China, 1997; p 77.
(31) Bond, A. M.; Miao, W. J.; Raston, C. L. *J. Phys. Chem. B* **2000**, *104*, 2320.
(32) Bond, A. M.; Miao, W. J.; Raston, C. L.; Sandoval, C. A. *J. Phys. Chem. B* **2000**, *104*, 8129.
(33) (a) Sheldrick, G. M. SHELXS-97, University of Gottingen, 1990. (b) Sheldrick, G. M SHELXL-97, University of Gottingen, 1997.
(34) Atwood, J. L.; Barbour, L. J.; Nichols, P. J.; Raston, C. L.; Sandoval, C. A. *Chem. Eur. J.* **1999**, *5*, 990.
(35) Atwood, J. L.; Barbour, L. J.; Raston, C. L.; Sudria, I. B. N. *Angew Chem. Int. Ed.* **1998**, *37*, 981.
(36) Raston, C. L.; Atwood, J. L.; Nichols, P. J.; Sudria, I. B. N. *Chem. Commun.* **1996**, 2615.
(37) Grey, I. E.; Hardie, M. J.; Ness, T. J.; Raston, C. L. *Chem. Commun.* **1999**, 1139.
(38) Crane, J. D.; Hitchcock, P. B. *J. Chem. Soc., Dalton Trans.* **1993**, 2537.
(39) Izuoka, A.; Tachikawa, T.; Sugawara, T.; Saito, Y.; Shinohara, H. *Chem. Lett.* **1992**, 1049.
(40) Andrews, P. C.; Atwood, J. L.; Barbour, L. J.; Nichols, P. J.; Raston, C. L. *Chem. Eur. J.* **1998**, *4*, 1384.
(41) Jehoulet, C.; Obeng, Y. S.; Kim, Y.-T.; Zhou, F.; Bard, A J. *J. Am. Chem. Soc.* **1992**, *114*, 4237.
(42) Chlistunoff, J.; Cliffel, D.; Bard, A. J. *Thin Solid Films* **1995**, *257*, 166.
(43) Bond, A. M.; Feldberg, S. W.; Miao, W.; Oldham, K. B.; Raston, C. L. *J. Electroanal. Chem.*, in press.
(44) Tatsuma, T.; Kikuyama, S.; Oyama, N. *J. Phys. Chem.* **1993**, *97*, 12067.
(45) Koh, W.; Dubois, D.; Kutner, W.; Jones, M. T.; Kadish, K. M. *J. Phys. Chem.* **1992**, *96*, 4163.
(46) Zhou, F.; Yau, S. L.; Jehoulet, C.; Laude, J. D. A.; Guan, Z.; Bard, A. J. *J. Phys. Chem.* **1992**, *96*, 4160.
(47) Compton, R. G.; Spackman, R. A.; Wellington, R. G.; Green, M. L. H.; Turner, J. *J. Electroanal. Chem.* **1992**, *327*, 337.
(48) Compton, R. G.; Spackman, R. A.; Riley, D. J.; Wellington, R. G.; Eklund, J. C.; Fisher, A. C.; Green, M. L. H.; Doothwaite, R. E.; Stephens, A. H. H.; Turner, J. *J. Electroanal. Chem.* **1993**, *344*, 235.